JOURNAL OF MATERIALS SCIENCE 29 (1994) 3419–3424

The influence of processing pressure on the formation of the high-T_c 2223 phase in Bi–Pb–Sr–Ca–Cu–O superconductors

G. GRABERT, G. H. HAERTLING
The Gilbert C. Robinson Department of Ceramic Engineering, Clemson University, Clemson, SC 29634, USA

The effects of processing pressure on the superconducting critical transition temperature, T_c, of $Bi_{1.6}Pb_{0.4}Sr_{1.9}Ca_{2.05}Cu_{3.05}O_x$ were investigated. Uniaxial cold- and hot-pressed samples prepared from mixed oxide and chemically coprecipitated powders were studied. The uniaxial cold-pressed specimens were pressed at a low pressure of 34.5 MPa (5000 p.s.i.) and a high pressure of 138.7 MPa (20 120 p.s.i.) and sintered at 845 °C for times ranging from 24–200 h. The mixed oxide samples showed a 0.5 K increase in T_c as the pressure was increased, while the chemically coprecipitated samples showed a 3.6 K increase in T_c with the same increase in pressure. The uniaxial hot-pressed specimens were hot pressed at 845 °C for 6 h in oxygen at a pressure of 34.5 MPa (5000 p.s.i.) and post-annealed for 24–30 h in air at 845 °C. These samples, both mixed oxide and chemically coprecipitated, showed an increase in T_c of approximately 25 K from the hot-pressed state to the post-annealed state. The highest T_c achieved by either of these processing methods was 108.4 K.

1. Introduction

Since the discovery of a high-T_c superconducting phase in the Bi–Sr–Ca–Cu–O (BSCCO) system by Maeda and his co-workers in January 1988 [1], extensive research has gone into the areas of processing, characterization, phase equilibria, physical property measurement, and device fabrication of these materials.

Processing the $Bi_2Sr_2Ca_2Cu_3O_x$ (2223 phase) superconductor has been especially attractive because of its (1) high T_c which is approximately 110 K, (2) lower oxygen stoichiometry sensitivity, (3) greater resistance to moisture degradation, and (4) it is less dangerous than the thallium-based superconductor. In addition, the difficulty in synthesizing the bulk material in phase-pure form has also attracted many investigators. The difficulty stems from the separation of the 2223 phase from the $Bi_2Sr_2Ca_1Cu_2O_x$ (2212) phase. The 2223 phase has a very small sintering temperature range and long sintering times are required to obtain bulk material which is almost phase-pure. Many investigators found it necessary to dope the BSCCO material with lead to achieve significant quantities of the 2223 phase. They showed that the lead increased the percentage of the 2223 phase formed and acted as a flux by decreasing the sintering temperature and time required to form the 2223 phase [2–8]. The lead was also shown to promote better crystallization. Another reason for doping the BSCCO material with lead is to increase the apparent valence of copper. As with the lanthanum-based system, the copper valence should be greater than 2 + . By replacing some of the Bi^{3+} with Pb^{2+}, the apparent valence of copper is increased. Some of these investigators believe that the Ca_2PbO_4 phase, excess CuO, different phases with the general formula $(Sr, Ca)_xCu_yO_z$, and the 2212 phase, all interact with one another by liquid-phase sintering, precipitation, or dissolution, to form the 2223 phase [8–19].

Pressure effects on the Y–Ba–Cu–O have been studied by several investigators [20–23]. In most of the studies, the pressure was applied to the Y–Ba–Cu–O specimens and the electrical properties were measured, primarily noting the effect of this applied pressure on $T_{c(onset)}$ and $T_{c(zero)}$. In the BSCCO materials, researchers have also used pressure as a means of increasing the critical current density, J_c, of the material through the use of hot pressing [24–27] and intermediate uniaxial pressing [28–31]. The pressure was used to increase the density of the compacts. This, in turn, reduced the weak links between the grains and, in some cases, gave preferential alignment of the grains in the a–b plane. Some of these researchers showed increases of two to three order of magnitude in J_c primarily due to the increased densities and improved intergrain contacts. It was also shown that post-annealing the hot-pressed compacts caused the J_cs to decrease. All of the samples were reported to consist of pure or nearly pure 2223 phase prior to pressure treatment.

2. Experimental procedure

Powders with the nominal composition $Bi_{1.6}Pb_{0.4}Sr_{1.9}Ca_{2.05}Cu_{3.05}O_x$ were prepared from

0022–2461

high-purity powder reagents using both the mixed-oxide and chemically coprecipitated routes. The starting materials in the mixed oxide route were Bi_2O_3 (Fisher Scientific, Pittsburgh, PA), PbO (Fisher Scientific, Pittsburgh, PA), $Sr(NO_3)_2$ (Mallinckrodt Paris, KY), $CaCO_3$ (Mallinckrodt Inc., Paris, KY), and CuO (Fisher Scientific, Pittsburgh, PA). These powders were weighed out and ball milled with distilled water for 1 h and dried at 100 °C for 18 h. The dried powders were then pressed into pellets and calcined once at 810 °C for 12 h and twice at 830 °C for 24 h in air. The pellets were ground using a mortar and pestle and repressed after each calcination step. For the chemically coprecipitated powder, the starting materials were $Bi(NO_3)_3$ (Mallinckrodt Inc., Paris, KY), in a dilute nitric acid solution, $Pb(NO_3)_2$ (Fisher Scientific, Pittsburgh, PA), Sr $(NO_3)_2$ (Mallinckrodt Inc., Paris, KY), $Ca(NO_3)_2 \cdot 4H_2O$ (Mallinckrodt Inc., Paris, KY), and $Cu(NO_3)_2 \cdot 2.5H_2O$ (Mallinckrodt Inc., Paris, KY). The bismuth nitrate solution was weighed out and poured into a beaker and the other constituents were added, one at a time, until each dissolved in the dilute nitric acid solution. Distilled water was added periodically to aid in this process. The solution was constantly stirred by a magnetic stirrer. After all the constituents were dissolved, a 20% excess aqueous solution of oxalic acid was added and stirred for 20 min. During this time, the pH was adjusted to approximately 3.5 with ammonium hydroxide. The solution was then dried in a vacuum oven for 12 h. After drying, the powder was heated to 600 °C for 2 h in an alumina crucible to burn off all the organic radicals. This precalcined powder was then ground and pressed into pellets and calcined at 830 °C for 12 h in air. The calcined powder was then ground with a mortar and pestle for processing. The pressing pressure for all calcination steps was 34.5 MPa (5000 p.s.i.). The heating rate used for calcination was 100 °C h^{-1} and the samples were furnace cooled.

To determine the influence of initial pressing pressure, half the samples were uniaxially cold pressed, using the calcined powders prepared from both the mixed oxide and chemically coprecipitated routes, at a low pressing pressure of 34.5 MPa (5000 p.s.i.), while the other half were uniaxially cold pressed at a higher pressing pressure of 138.7 MPa (20 120 p.s.i.). The pellets were then sintered at 845 °C in air. The mixed oxide pellets were sintered for times ranging from 20–200 h, while the chemically coprecipitated pellets were sintered for 24–30 h. These conditions were selected in order to maximize the formation of the 2223 phase and to aid in the determination of pressure influence. These materials were then electroded and tested. The heating and cooling rates for sintering were the same as those used for calcination. In the determination of pressure influence throughout sintering, the calcined powders were uniaxially hot pressed at 845 °C in oxygen for 6 h at a pressure of 34.5 MPa (5000 p.s.i.). Half of these compacts were then subjected to an additional heat treatment in a conventional electric furnace at 845 °C for 24–30 h in air. These materials were then electroded and tested.

The critical temperature and critical current density were evaluated using a standard four-point method. The resistance was measured by a Keithley, Model 580, micro-ohmmeter with a sensitivity of 10^{-6} Ω. The critical currents were measured using a 1 μV mm^{-1} standard by a Keithley, Model 197, Autoranging Micro Volt DMM. In addition, the structures of the samples were examined by powder X-ray diffraction (XRD) using CuK_α radiation (Scintag XDS 2000). Scanning electron microscopy (SEM) equipped with an energy dispersive X-ray analysis (EDAX) unit (Jeol JSM/IC 848 scanning electron microscope) and optical microscopy (OM) (Zeiss ICM 405) were used to observe the homogeneity and surface morphology of the materials. A BET surface area analyser (Micromeritics Gemini 2360) and a sedigraph (Micromeritics 5100) were used to determine the particle size and distribution of the BSCCO materials. Differential thermal analysis (DTA) (Perkin–Elmer DTA 1700 differential thermal analyser) was used to determine the thermal effects of the BSCCO materials. The electrodes for all materials were applied using a commercial silver paste, C8710 from Heraeus Inc., Cermalloy Division, and fired at 845 °C for 18 min.

3. Results and discussion

The samples prepared by the mixed oxide route required sintering times in excess of 200 h to obtain materials which were nearly pure 2223 phase. The X-ray powder diffraction analysis confirmed the existence of the 2223 phase with small impurities of Ca_2PbO_4 and Ca_2CuO_3 after 200 h sintering. The T_c of this material was 108.1 K. The average particle size of the calcined mixed oxide powder was 15 μm and the green density of the pellet pressed from the powder at 34.5 MPa (5000 p.s.i.) was 4.23 g cm^{-3}. When the pressing pressure was increased to 138.7 MPa (20 120 p.s.i.), the green density increased to 4.95 g cm^{-3}. Fig. 1 shows the resistance versus temperature curves for the mixed oxide pellets uniaxially cold pressed both at the high and low pressures and sintered at 845 °C for 125 h in air. The high-pressure compact had a T_c of 107.3 K while that

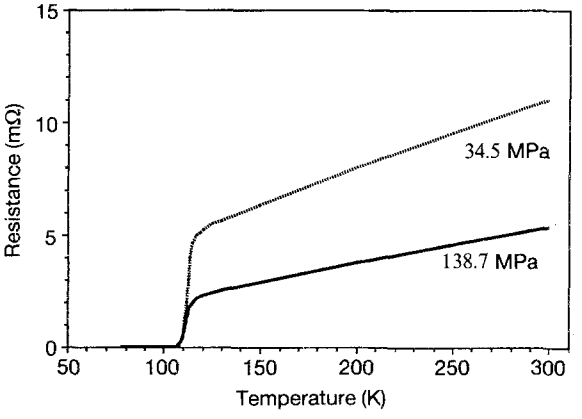

Figure 1 Resistance versus temperature curves for mixed-oxide pellets pressed at different initial pressures and sintered at 845 °C for 125 h in air.

of the low-pressure compact was 0.5 K lower at 106.8 K. This may have, at first, seemed to be a trivial difference in T_c until the approximate sintering time required for the low-pressure compact to reach the T_c of 107.3 K was determined. Fig. 2 shows the sintering time versus critical temperature plot for the mixed oxide compacts uniaxially cold pressed at 34.5 MPa (5000 p.s.i.) and sintered at 845 °C in air for times ranging from 20–200 h. Also shown in Fig. 2 is a point from the 138.7 MPa (20 120 p.s.i.) high-pressure compact sintered at 845 °C for 125 h in air. The other point on the plot is the approximate sintering time required to achieve the 107.3 K using the lower starting pressure. This approximate value is 155 h, which means the low-pressure compact would require an additional 30 h sintering to achieve the higher T_c. This increase in T_c with increased pressing pressure was believed to be due primarily to the increase in density, which increased the number of particle to particle contacts, thus making the material more reactive. This increase in the particle to particle contacts enhanced the formation of the high T_c 2223 phase and allowed the sintering times to be reduced. Referring again to Fig. 1, another interesting aspect of the difference in pressing pressure was a reduction in room-temperature resistivity by approximately half, from the low-pressure compact to the high pressure one. This effect was also believed to be due to the increase in density and reactivity. The other aspects of the two curves were basically similar. The transition widths were approximately the same for both curves, and they showed a decrease in resistivity with a sharp drop to zero starting around 120 K. The microstructure of both pellets can be seen from scanning electron micrographs shown in Fig. 3. The high-pressure compact was much more dense and appeared to have a higher degree of grain alignment when compared to that of the low-pressure compact.

The chemically coprecipitated powders were much more homogeneous and reactive than those of the mixed oxide powders. In addition, the average particle size for the chemically coprecipitated powders was 3 μm. The green densities were approximately the same as those for the mixed oxide powders, however, the fired densities were higher. The relative fired density for the chemically coprecipitated compact was approximately 84% (5.3 g cm^{-3}) while that of the mixed oxide compact was only around 75% (4.8 g cm^{-3}). Fig. 4 shows the resistance versus temperature curves for the chemically coprecipitated pellets uniaxially cold pressed, both at the high and low pressures and sintered at 845 °C for 30 h in air. As was the case for the mixed oxide samples, the room-temperature resistivities of the high pressing pressure compacts was lower than that of the low pressing pressure compacts. Overall, the resistivities for the chemically coprecipitated pellets were found to be much lower than those of the mixed-oxide pellets. Both of the curves in Fig. 4 decreased in resistance with decreasing temperature, but the onset of superconductivity was 123 K, which was slightly higher for these materials compared with the mixed-oxide pellets. The biggest difference between the two methods was the sintering time required to form the nearly pure 2223 phase. The mixed-oxide route required sintering times six to seven times longer than the chemically coprecipitated materials. The increased pressing pressure also increased the T_c of the materials but this time by 3.6 K. The microstructure of the chemically coprecipitated material, as shown from the scanning electron micrographs in Fig. 5, had the same flaky

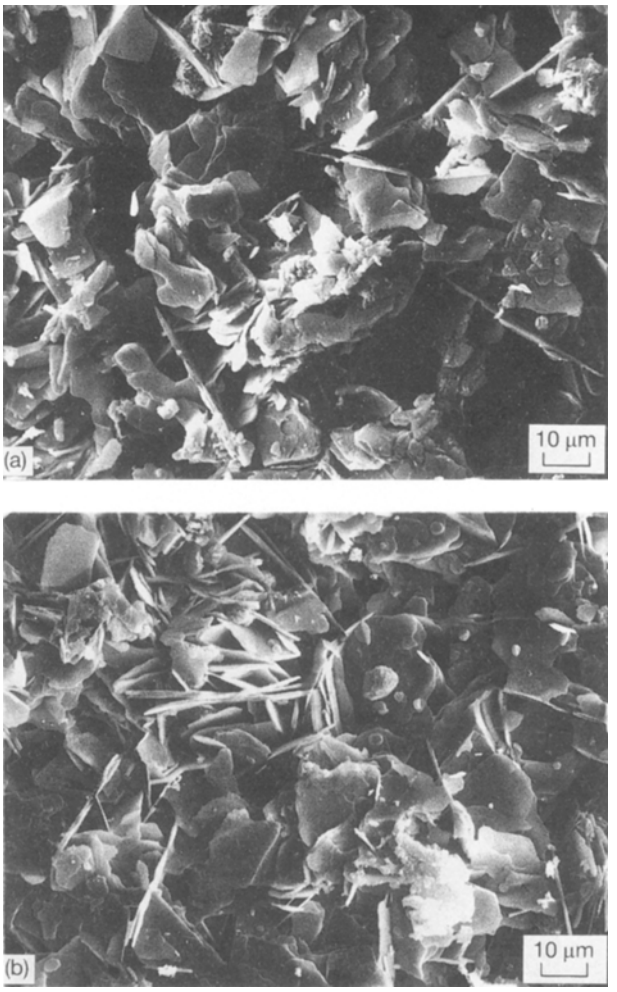

Figure 3 Scanning electron micrographs for mixed oxide pellets pressed at (a) 34.5 MPa (5000 p.s.i.), and (b) 138.7 MPa (20 120 p.s.i.) and sintered at 845 °C for 125 h in air.

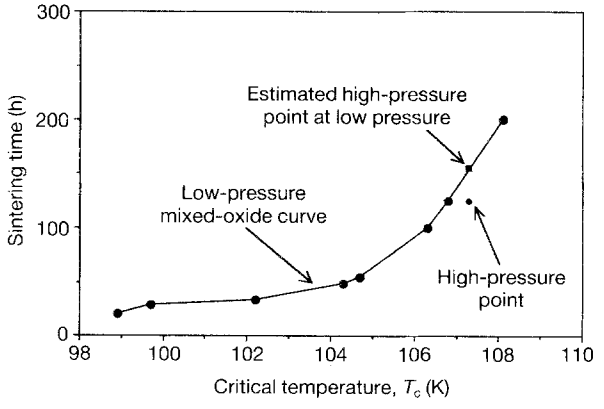

Figure 2 Sintering time versus critical temperature plot showing the effect of initial pressing pressure on the T_c.

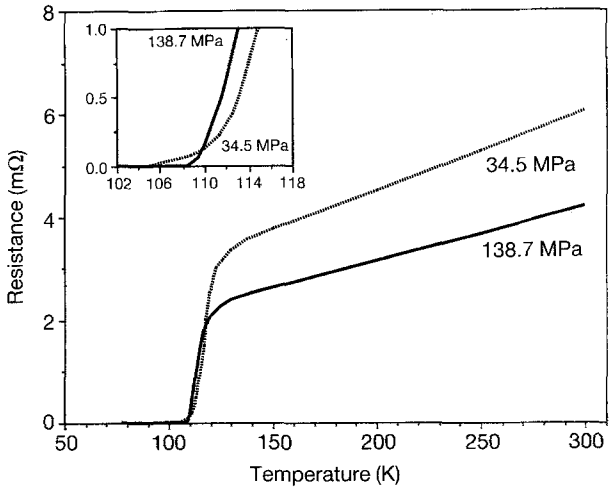

Figure 4 Resistance versus temperature curves for coprecipitated pellets pressed at different initial pressures and sintered at 845 °C for 30 h in air.

Figure 5 Scanning electron micrographs for coprecipitated pellets pressed at (a) 34.5 MPa (5000 p.s.i.), and (b) 138.7 MPa (20 120 p.s.i.) and sintered at 845 °C for 30 h in air.

behaviour as the mixed-oxide materials but the grain size is now much smaller and the compact much more dense. Similarly, the high-pressure compact was much more dense and had a much higher degree of orientation when compared with the low-pressure compact. A closer look at the high-pressure compact shows that there was actually some partial melting taking place, and this definitely contributed to the higher densities and increased T_cs. This also shows that sintering was aided by the presence of the liquid phase and this increased the rate of formation of the high T_c 2223 phase.

Because initial pressing pressure has shown to be effective in increasing the density and developing grain-oriented microstructures, the effectiveness of pressure throughout sintering was investigated via hot pressing. It was believed that hot pressing would intensify the effects seen from the increased pressing pressure. Fig. 6 shows the resistance versus temperature curves for uniaxial hot-pressed mixed oxide compacts which were prepared at 845 °C for 6 h in oxygen at 34.5 MPa (5000 p.s.i.), with and without a post-anneal at 845 °C for 24 h in air. The as-hot-pressed sample showed that the material had a sharp transition to the superconducting state at 83.3 K. The X-ray powder diffraction analysis showed this material to be primarily composed of the 2212 phase. When the material was post-annealed, the T_c increased by approximately 25 K to a T_c of 108.2 K. The phase was almost entirely converted to the 2223 phase. In addition, the resistivity dropped by an order of magnitude from the hot-pressed state to the post-annealed state. Although the chemically coprecipitated powder was much more reactive, homogeneous and had a finer particle size, the results of the chemically coprecipitated material were the same as those for the mixed-oxide samples. The microstructures of the as-hot-pressed sample and the post-annealed one can be seen in Fig. 7. The as-hot-pressed sample appears to be a very dense melt with partial orientation, but when the material was post-annealed, the density dropped from about 97% to about 92% relative density. The grains actually appeared to grow right out of the melt to give the appearance of a very open structure. This could be a little deceiving, but this material was still much more dense than any of those produced by the increase in initial pressing pressure. The high T_c 2223 phase of the mixed-oxide samples was shown to be formed in a much less time when hot-pressed and post-annealed as

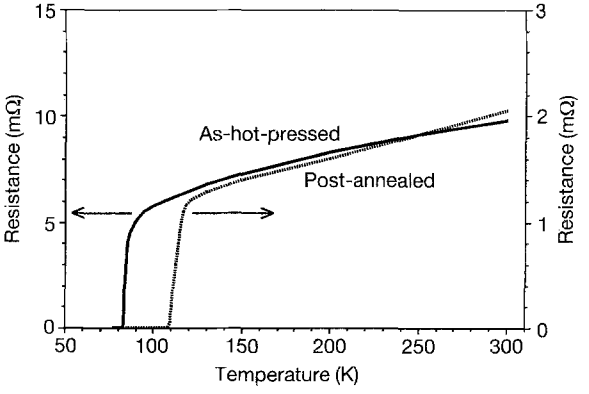

Figure 6 Resistance versus temperature curves for coprecipitated compacts hot-pressed at 34.5 MPa (5000 p.s.i.) in oxygen at 845 °C for 6 h. One of the compacts was post-annealed at 845 °C for 24 h in air.

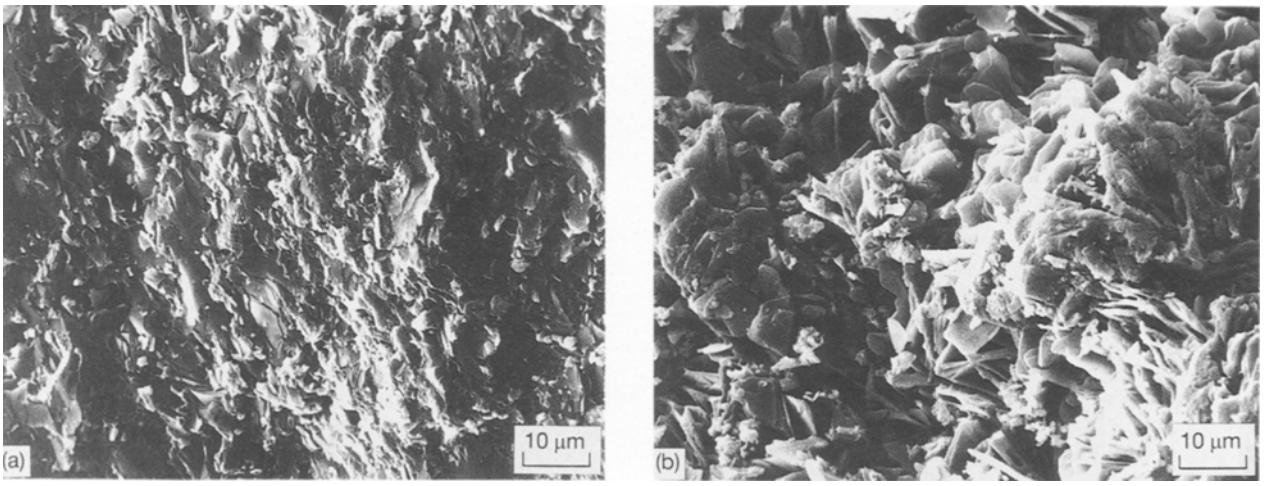

Figure 7 Scanning electron micrographs for coprecipitated pellets (a) as-hot-pressed and (b) hot-pressed and post-annealed.

opposed to the material just being sintered. In contrast, the chemically coprecipitated materials could be used to form the high T_c phase in the same amount of time by either method. The pressure throughout sintering had a similar effect to that of the processing pressure, in that the density of these materials increased and the grains became more oriented. The increased density caused an increase in the number of particle to particle contacts which increased the reactivity and these together decreased the amount of time required to form the high T_c 2223 phase.

4. Conclusions

Higher pressing pressures have been shown to produce materials which have better electrical properties than those produced from the lower pressing pressures. The mixed-oxide samples showed a 0.5 K increase in T_c as the pressure was increased, and the chemically coprecipitated samples showed a 3.6 K increase in T_c with the same increase in pressure. The chemically coprecipitated powder is preferred over the mixed-oxide powder because a larger percentage of the high T_c 2223 phase can be formed in much less time. The hot-pressed samples, both mixed-oxide and chemically coprecipitated, showed an increase in T_c of approximately 25 K from the as-hot-pressed condition to the post-annealed condition. The hot-press with post-anneal enhanced the formation of the 2223 phase for the mixed oxide materials by reducing the sintering time required to form a nearly phase-pure material. This shows the influence that pressure has on the conversion of the lower T_c phase to the higher T_c phase. The higher pressure causes conversion in a substantially shorter amount of time due to the compact being much more dense and uniform. The initial pressing pressure and the pressure throughout sintering had similar effects on the BSCCO materials, in that the increased pressure increased the density of these materials and the grains became more oriented. The increased density caused an increase in the number of particle to particle contacts which increased the reactivity of the materials. This could be due to the sliding and/or breaking up of particles for increased particle packing. All together, the higher pressures decreased the amount of time required to form the high T_c 2223 phase and increased the critical transition temperature.

Acknowledgements

The authors wish to express their sincere thanks to Dr Dennis R. Dinger for his valuable discussion and Dr John D. Buckley for his support. The authors also thank JoAn Hudson, Andy Nelson, Robert Ball and Shannon Baldwin of the Clemson University Electron Microscope Facility, for their assistance in preparation of the scanning electron micrographs. This work was funded by a grant from NASA-Langley Research Center (Contract NAG-1-1108).

References

1. H. MAEDA, Y. TANAKA, M. FUKUTOMI and T. ASANO, *Jpn J. Appl. Phys.* **27** (1988) L209.
2. R. B. TRIPATHI and D. W. JOHNSON Jr, *J. Am. Ceram. Soc.* **74** (1991) 247.
3. M. TAKANO, J. TAKADA, K. ODA, H. KITAGUCHI, Y. MIURA, Y. IKEDA, Y. TOMII and H. MAZAKI, *Jpn J. Appl. Phys.* **27** (1988) L1041.
4. Y. YAMADA and S. MURASE, *ibid.* **27** (1988) L996.
5. M. MIZUNO, H. ENDO, J. TSUCHIYA, N. KIJIMA, A. SUMIYAMA and Y. OGURI, *ibid.* **27** (1988) L1225.
6. K. TOGANO, H. KUMAKURA, H. MAEDA, E. YANAGISAWA and K. TAKAHASHI, *Appl. Phys. Lett.* **53** (1988) 1329.
7. S. NARUMI, H. OHTSU, I. IGUCHI and R. YOSHIZAKI, *Jpn J. Appl. Phys.* **28** (1989) L27.
8. C. J. KIM, C. K. RHEE, H. G. LEE, S. J-L. KANG and D. Y. WON, *ibid.* **28** (1989) L45.
9. Y. L. CHEN and R. STEVENS, *J. Am. Ceram. Soc.* **75** (1992) 1150.
10. W. WONG-NG, C. K. CHIANG, S. W. FREIMAN, L. P. COOK and M. D. HILL *Am. Ceram. Soc. Bull.* **78** (1992) 1261.
11. A. OOTA, K. OHBA, A. ISHIDA, A. KIRIHIGASHI, K. IWASAKI and H. KUWAJIMA, *Jpn J. Appl. Phys.* **28** (1989) L1171.
12. Y. OKA, N. YAMAMOTO, H. KITAGUCHI, K. ODA and J. TAKADA, *ibid.* **28** (1989) L213.
13. H. SASAKURA, S. MINAMIGAWA, K. NAKAHIGASHI, M. KOGACHI, S. NAKANISHI, N. FUKUOKA, M. YOSHIKOWA, S. NOGUCHI, K. OKUDA and A. YANASE, *ibid.* **28** (1989) L1163.

14. Y. T. HUANG, W. N. WANG, S. F. WU, C. Y. SHEI, W. M. HURNG, W. H. LEE and P. T. WU, *J. Am. Ceram. Soc.* **73** (1990) 3507.
15. F. H. CHEN, H. S. KOO and T. Y. TSENG, *Appl. Phys. Lett.* **58** (1991) 637.
16. N. KIJIMA, H. ENDO, J. TSUCHIYA, A. SUMIYAMA, M. MIZUNO and Y. OGURI, *Jpn J. Appl. Phys.* **27** (1988) L1852.
17. Y. T. HUANG, R. G. LIU, S. W. LU, P. T. WU and W. N. WANG, *Appl. Phys. Lett.* **56** (1990) 779.
18. K. H. YOON and H. B. LEE, *J. Mater. Sci.* **26** (1991) 5101.
19. T. HATANO, K. AOTA, S. IKEDA, K. NAKAMURA and K. OGAWA, *Jpn J. Appl. Phys.* **27** (1988) L2055.
20. P. H. HOR, L. GAO, R. L. MENG, Z. J. HUANG, Y. Q. WANG, K. FOSTER, J. VASILIONS, C. W. CHU, M. K. WU, J. R. ASHBURN and J. TORNG, *Phys. Rev. Lett.* **58** (1987) 911.
21. H. YOSHIDA, H. MORITA, K. NOTO, T. KANEKO and H. FUJIMORI, *Jpn J. Appl. Phys.* **26** (1987) L867.
22. K. MURATA, H. IHARA, M. TOKUMOTO, M. HIRABAYASHI, N. TERADA, K. SENZAKA and Y. KIMURA, *ibid.* **26** (1987) L471.
23. A. DRIESSEN, R. GRIESSEN, N. KOEMAN, E. SALOMONS, R. BROUWER, D. G. DEGROOT, K. HEECK, H. HEMMES and J. RECTOR, *Phys. Rev. B* **36** (1988) 5602.
24. H. IKEDA, R. YOSHIZAKI, K. YOSHIKAWA and N. TOMITA, *Jpn J. Appl. Phys.* **29** (1990) L430.
25. R. YOSHIZAKI, H. IKEDA, K. YOSHIKAWA and N. TOMITA, *ibid.* **29** (1990) L753.
26. H. ENAMI, N. KAWAHARA, T. SHINOHARA, S. KAWABATA, H. HOSHIZAKI, A. MATSUMURO and T. IMURA, *ibid.* **28** (1989) L377.
27. K. H. SONG, C. C. SORRELL, S. X. DOU and H. K. LIU, *J. Am. Ceram. Soc.* **74** (1991) 2577.
28. T. ASANO, Y. TANAKA, M. FUKUTOMI, K. JIKIHARA, J. MACHIDA and H. MAEDA, *Jpn J. Appl. Phys.* **27** (1988) L1652.
29. Y. TANAKA, T. ASANO, K. JIKIHARA, M. FUKUTOMI, J. MACHIDA and H. MAEDA, *ibid.* **27** (1988) L1655.
30. T. ASANO, Y. TANAKA, M. FUKUTOMI, K. JIKIHARA and H. MAEDA, *ibid.* **28** (1989) L595.
31. A. ITO, M. MATSUDA, Y. IWAI, M. ISHII, M. TAKATA, T. YAMASHITA and H. KOINUMA, *ibid.* **28** (1989) L380.

Received 22 June 1993
and accepted 10 January 1994